Journal of Geodesy (2001) 75: 491–504

Journal of Geodesy

Effects of the spherical terrain on gravity and the geoid

P. Novák[1], P. Vaníček[1], Z. Martinec[2], M. Véronneau[3]

[1] Department of Geodesy and Geomatics Engineering, University of New Brunswick, PO BOX 4400, Fredericton, E3B 5A3 Canada
[2] Department of Geophysics, Charles University, V Holešovičkách 2, 180 00 Praha 8, Czech Republic
[3] Geodetic Survey Division, Natural Resources Canada, 615 Booth Street, Ottawa, K1A 0E9 Canada

Received: 16 June 2000 / Accepted: 27 April 2001

Abstract. The determination of the gravimetric geoid is based on the magnitude of gravity observed at the topographical surface and applied in two boundary value problems of potential theory: the Dirichlet problem (for downward continuation of gravity anomalies from the topography to the geoid) and the Stokes problem (for transformation of gravity anomalies into the disturbing gravity potential at the geoid). Since both problems require involved functions to be harmonic everywhere outside the geoid, proper reduction of gravity must be applied. This contribution deals with far-zone effects of the global terrain on gravity and the geoid in the Stokes–Helmert scheme. A spherical harmonic model of the global topography and a Molodenskij-type spectral approach are used for a derivation of suitable computational formulae. Numerical results for a part of the Canadian Rocky Mountains are presented to illustrate the significance of these effects in precise (i.e. centimetre) geoid computations. Their omission can be responsible for a long-frequency bias in the geoid, especially over mountainous areas. Due to the rough topography of the testing area, these numerical values can be used as maximum global estimates of the effects (maybe with the exception of the Himalayas). This study is a continuation of efforts to model adequately the topographical effects on gravity and the geoid, especially of a comparing the effects of the planar topographical plate and the spherical topographical shell on gravity and the geoid [Vaníček, Novák, Martinec (2001) J Geod 75: 210–215].

Key words: Gravimetric Geoid – Helmert's Reduction of Gravity – Spherical Terrain Effects

Correspondence to: P. Novák
Department of Geomatics Engineering,
The University of Calgary, 2500 University Drive NW,
Calgary, T2N 1N4 Canada
e-mail: pnovak@ucalgary.ca
Tel.: +1-403-617-9157
Fax: +1-403-284-1980

1 Introduction

Vaníček et al. (2001) discussed significant differences in magnitude of the topographical effects on gravitational potential and gravitational acceleration generated by an infinite planar plate and a global spherical shell. This manuscript was submitted separately because it focuses on something quite different and only incidentally forms a foundation for the present contribution. Two basic conclusions of Vaníček et al.'s investigation, relevant for this contribution, can be summarized as follows: although the choice of either the plate or the shell does not significantly effect the classical Bouguer reduction of gravity, it has rather important consequences for the harmonization of the Earth's gravity field above the geoid which disqualifies the plate model from its use in precise geoid computations. The effects discussed in Vaníček et al. (2001) represent an approximation of first order which must be corrected for all deviations of the actual topography from the spherical shell, referred to as a terrain. In the following, we aim to discuss the spherical terrain effects on gravity and the consequences of their adoption for the geoid. When speaking about the spherical model of topography (terrain), we really mean the spherical approximation of the geoid from which topographical masses are defined.

2 Topographical effects in the Stokes–Helmert scheme

The effect of topography in the context of the Stokes–Helmert approach (Heck 1992; see also Vaníček and Martinec 1994) is evaluated in terms of three separate effects: the direct topographical effect (DTE) on gravity, the primary indirect topographical effect (PITE) on the geoid, and the secondary indirect topographical effect (SITE) on gravity. These three topographical effects can easily be defined using the Helmert disturbing gravity potential T^{h}, which is related to the disturbing gravity potential T of the Earth's gravity field as follows [Martinec et al. 1993, Eq. (8)]:

$$T^{\mathrm{h}}(r,\Omega) = T(r,\Omega) - \delta V^{\mathrm{t}}(r,\Omega) \tag{1}$$

A triplet of the curvilinear coordinates $(r,\varphi,\lambda) = (r,\Omega)$ defines a position of the computation point in the geocentric spherical coordinate system. The parameter δV^{t} is the residual topographical potential, which can be defined as a sum of the potential of the Bouguer shell, plus the potential of the terrain, minus the potential of the condensed Bouguer shell, minus the potential of the condensed terrain [Martinec 1998, Eqs. (3.12) and (3.26)]. Values of the function T^{h} at the geoid (approximated in the following by the reference sphere of radius R) are solved for in the Stokes–Helmert scheme. The geoid N and the PITE on the geoid P can then be derived from Eq. (1) by the spherical Bruns theorem as follows:

$$N(\Omega) = \frac{T^{\mathrm{h}}(R,\Omega) + \delta V^{\mathrm{t}}(R,\Omega)}{\gamma} = \frac{T^{\mathrm{h}}(R,\Omega)}{\gamma} + P(\Omega) \tag{2}$$

where γ is normal gravity at the reference ellipsoid. Applying the negative radial derivative to Eq. (1), we obtain the corresponding topographical effects on gravity

$$\delta g^{\mathrm{h}}(r,\Omega) = \delta g(r,\Omega) + \frac{\partial\ \delta V^{\mathrm{t}}(r,\Omega)}{\partial r}\bigg|_r \tag{3}$$

where symbols δg and δg^{h} stand for gravity disturbances defined in the real and the Helmert gravity fields. Since gravity disturbances δg differ from gravity anomalies Δg only by a vertical change of normal gravity along the separation between the actual equipotential surface (real or Helmert) and the equivalent normal equipotential surface, we obtain for the spherical approximation of a vertical gradient of normal gravity the following expression (Vaníček et al. 1999, Sect. 3):

$$\Delta g^{\mathrm{h}}(r,\Omega) + \frac{2}{R}T^{\mathrm{h}}(r,\Omega) = \Delta g(r,\Omega) + \frac{2}{R}T(r,\Omega) + \frac{\partial\,\delta V^{\mathrm{t}}(r,\Omega)}{\partial r}\bigg|_r \tag{4}$$

Equation (4) can easily be re-arranged using the DTE on gravity, D, and the SITE on gravity, S,

$$\begin{aligned}\Delta g^{\mathrm{h}}(r,\Omega) &= \Delta g(r,\Omega) + \frac{2}{R}\delta V^{\mathrm{t}}(r,\Omega) + \frac{\partial \delta V^{\mathrm{t}}(r,\Omega)}{\partial r}\bigg|_r \\ &= \Delta g(r,\Omega) + S(r,\Omega) + D(r,\Omega)\end{aligned} \tag{5}$$

We will then discuss these three effects sequentially.

3 The direct topographical effect on gravity

The spherical form of the DTE was formulated by Martinec and Vaníček (1994a). The DTE can be evaluated as a sum of the effect of the Bouguer shell A^{b}, plus the effect of the terrain A^{t}, minus the effect of the condensed Bouguer shell A^{cb}, minus the effect of the condensed terrain A^{ct}

$$\begin{aligned}D(R+H,\Omega) = {} & A^{\mathrm{b}}(R+H,\Omega) + A^{\mathrm{t}}(R+H,\Omega) \\ & - A^{\mathrm{cb}}(R+H,\Omega) - A^{\mathrm{ct}}(R+H,\Omega)\end{aligned} \tag{6}$$

All terms in Eq. (6) are related to the topography of the geocentric radius $R+H$, where H is the orthometric height of topography. We will deal only with the two terrain effects, A^{t} and A^{ct}, as the other two effects were discussed in Vaníček et al. (2001). Since the effects A^{b} and A^{cb} cancel each other if the mass conservation scheme is used (Wichiencharoen 1982), the difference $D^{\mathrm{ter}} = A^{\mathrm{t}} - A^{\mathrm{ct}}$, called in the following the 'direct terrain effect' (DTerE), accounts for the entire DTE on gravity.

It was shown by Martinec and Vaníček (1994a) that for the evaluation of this difference – they called it the roughness term – it does not matter which of the condensation schemes is used. Different condensation schemes were discussed by, for instance, Wichiencharoen (1982) (see also Vaníček et al. 2001). Here, the mass conservation scheme only will be deployed. D^{ter} is then given by the following formula (Martinec and Vaníček 1994a):

$$\begin{aligned}D^{\mathrm{ter}}&(R+H,\Omega) \\ &= G\varrho_{\mathrm{o}}^{\mathrm{t}} \iint_{\Omega_\oplus} \frac{\partial}{\partial r} \int_{\xi=R+H(\Omega)}^{R+H(\Omega')} \mathscr{L}^{-1}(r,\psi,\xi)\xi^2\,\mathrm{d}\xi\bigg|_{r=R+H(\Omega)} \mathrm{d}\Omega' \\ &\quad - G\varrho_{\mathrm{o}}^{\mathrm{t}} \iint_{\Omega_\oplus} \int_{\xi=R+H(\Omega)}^{R+H(\Omega')} \xi^2\,\mathrm{d}\xi \\ &\quad \times \frac{\partial}{\partial r}\mathscr{L}^{-1}(r,\psi,R)\bigg|_{r=R+H(\Omega)} \mathrm{d}\Omega'\end{aligned} \tag{7}$$

Here, G stands for the universal gravitational constant, $\varrho_{\mathrm{o}}^{\mathrm{t}}$ is the mean topographical density, ξ is the integration parameter, and $\Omega_\oplus$ is the full spatial angle. The Newtonian integration kernel $\mathscr{L}^{-1}$ in Eq. (7) is of the form

$$\mathscr{L}^{-1}(r,\psi,\xi) = \left(r^2 + \xi^2 - 2r\,\xi\cos\psi\right)^{-\frac{1}{2}} \tag{8}$$

where ψ is a spherical distance between the geocentric directions $\Omega = (\varphi,\lambda)$ and $\Omega' = (\varphi',\lambda')$ which can easily be computed by the law of cosines as follows:

$$\cos\psi = \cos\varphi\cos\varphi' + \sin\varphi\sin\varphi'\cos(\lambda-\lambda') \tag{9}$$

We will now show that, contrary to our earlier belief, it is not possible to stop integrating at a small value of the cap radius (i.e. truncation of the integration domain $\Omega_\oplus$ to a spherical cap of radius ψ_{o} equal to 1°, 3° or 5°). To show this, we can evaluate each of the two integrals in Eq. (7) in two parts: the integral over the spherical cap of radius ψ_{o}, i.e. $0 < \psi < \psi_{\mathrm{o}}$ (near-zone contribution), and the integral over the rest of the world, i.e. $\psi_{\mathrm{o}} \le \psi \le \pi$ (far-zone contribution). The integral over the near zone can clearly be evaluated from the available DTM through a standard 2-D numerical integration

using the discretized form of the corresponding integrals (e.g. by the Gaussian quadrature rule); see, for example, Novák (2000). As this is a fairly standard procedure (integration is replaced according to the mean-value theorem by discrete summation), we will not discuss it any further here. The far-zone contribution is a different matter all together; it must be evaluated using a different approach.

In order to obtain the far-zone contribution to the first integral in Eq. (7), we expand the spatial form of the integral

$$\frac{\partial}{\partial r}\int_{\xi=R+H(\Omega)}^{R+H(\Omega')} \mathscr{L}^{-1}(r,\psi,\xi)\xi^2\,\mathrm{d}\xi\Bigg|_{r=R+H(\Omega)} \tag{10}$$

to its spectral form. This is done by means of the technique introduced by Molodenskij et al. (1960), which yields (see Appendix A)

$$2\pi G\varrho_{\mathrm{o}}^{\mathrm{t}}\left[\sum_{n=0}^{nh1} t_n(\psi,\psi_o)H_n(\Omega) - \frac{2H(\Omega)}{R+H(\Omega)}\sum_{n=0}^{nh1} u_n(\psi,\psi_{\mathrm{o}}) \times H_n(\Omega) + \frac{1}{R+H(\Omega)}\sum_{n=0}^{nh2} v_n(\psi,\psi_o)H_n^2(\Omega) + \mathcal{O}\left(\frac{H_n^3}{R^2}\right)\right] \tag{11}$$

For the far-zone contribution to the second integral in Eq. (7), we obtain similarly (see Appendix A)

$$2\pi G\varrho_{\mathrm{o}}^{\mathrm{t}}\left[\sum_{n=0}^{nh1} w_n(H,\psi,\psi_{\mathrm{o}})H_n(\Omega) + \frac{1}{R}\sum_{n=0}^{nh2} w_n(H,\psi,\psi_{\mathrm{o}})\,H_n^2(\Omega) + \mathcal{O}\left(\frac{H_n^3}{R^2}\right)\right] \tag{12}$$

Coefficients t_n, u_n, v_n and w_n are the Molodenskij truncation coefficients (weights) defined in Appendix A [see Eqs. (A14)–(A17)]. Zonal coefficients H_n for the spherical harmonic representation of heights in Eqs. (11) and (12) to their maximum available degree $nh1$ can be computed from a global elevation model such as TUG87 (Wieser 1987)

$$H_n(\Omega) = \sum_{m=-n}^{n} H_{n,m}Y_{n,m}(\Omega) \quad \forall\, n = 0,\ldots,nh1 \tag{13}$$

and the corresponding coefficients H_n^2 for squared heights

$$H_n^2(\Omega) = \sum_{m=-n}^{n} H_{n,m}^2 Y_{n,m}(\Omega), \quad \forall\, n = 0,\ldots,nh2 \tag{14}$$

$Y_{n,m}$ stands for the Laplace spherical harmonics (Heiskanen and Moritz 1967). Maximum degrees of $nh1 = 180$ and $nh2 = 90$ were used in our computations.

The far-zone contribution to the DTerE is given by the difference of the series of Eqs. (11) and (12)

$$\begin{aligned} D^{\mathrm{ter}}(R+H,\Omega) &= 2\pi G\varrho_{\mathrm{o}}^{\mathrm{t}}\left[\sum_{n=0}^{nh1} t_n(\psi,\psi_{\mathrm{o}})H_n(\Omega) - \frac{2H(\Omega)}{R+H(\Omega)}\right. \\ &\quad\times\sum_{n=0}^{nh1} u_n(\psi,\psi_{\mathrm{o}})H_n(\Omega) + \frac{1}{R+H(\Omega)}\sum_{n=0}^{nh2} v_n(\psi,\psi_{\mathrm{o}})H_n^2(\Omega) \\ &\quad - \sum_{n=0}^{nh1} w_n(H,\psi,\psi_{\mathrm{o}})H_n(\Omega) - \frac{1}{R}\sum_{n=0}^{nh2} w_n(H,\psi,\psi_{\mathrm{o}})H_n^2(\Omega) \\ &\quad \left.+\,\mathcal{O}\left(\frac{H_n^3}{R^2}\right)\right], \quad \forall\,\psi \geq \psi_{\mathrm{o}} > 0 \end{aligned} \tag{15}$$

The terms of the order H_n cancel eventually each other after expanding $H(\Omega)$ into a series form. The same would apply to Eqs. (21) and (26). For our test area (see Fig. 1), selected to cover the most challenging part of the Canadian Rocky Mountains, and for $\psi_{\mathrm{o}} = 3°$, we obtain the numerical results shown in Fig. 2. Clearly, in the mountains, the effect of the far zone is very significant even for a relatively large near zone, so that it certainly cannot be neglected. Our further computations (not given here) have shown that the far-zone effect is similarly significant for the whole territory of Canada and cannot be neglected anywhere, if an accurate geoid is to be computed. It must be noted that the far-zone contribution is of a long-wavelength character. Continuing these values down to the geoid and applying Stokes' integration, corresponding effects on the geoid can be obtained (see Fig. 3). The range of both values, including basic statistical parameters (mean and standard deviation), is shown in Tables 1 and 2.

Another spherical harmonic expression for the DTE on gravity up to order H_n^3 was derived by Nahavandchi and Sjöberg [1998, Eq. (20)], expanding the Newtonian kernel into a series of Legendre polynomials. To account for a near-zone terrain, a new formula, representing a compromise between the local integration and the spherical harmonic expression was derived in Nahavandchi [2000, Eq. (21)].

4 The primary indirect topographical effect on the geoid

The mathematical expression for the spherical form of the PITE on the geoid was derived by Martinec and Vaníček (1994b). This effect is merely a re-scaled value (by normal gravity) of the residual topographical potential evaluated at the reference sphere, see Eq. (2). Following the same approach as that we applied for the DTE, this effect can be evaluated as a sum of the effect of the Bouguer shell P^{b}, plus the effect of the terrain P^{t}, minus the effect of the condensed Bouguer shell P^{cb}, minus the effect of the condensed terrain P^{ct}

$$P(\Omega) = P^{\mathrm{b}}(\Omega) + P^{\mathrm{t}}(\Omega) - P^{\mathrm{cb}}(\Omega) - P^{\mathrm{ct}}(\Omega) \tag{16}$$

All terms are related to the reference sphere of radius R which approximates the geoid. The Bouguer shell effects

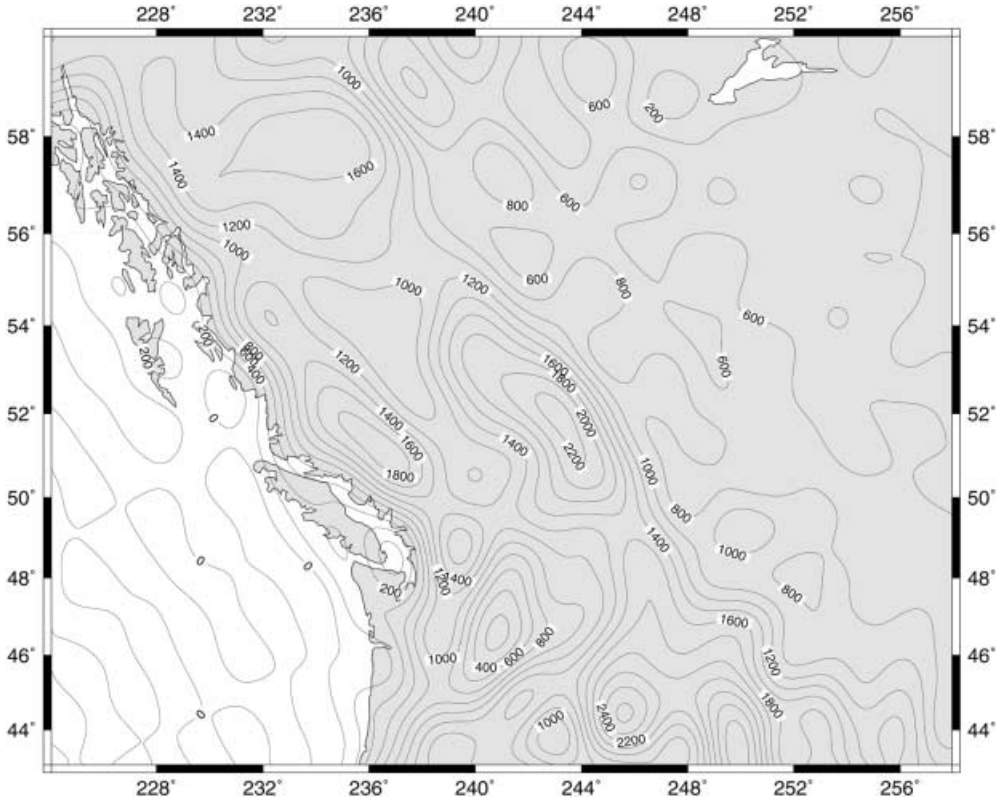

Fig. 1. Spectral topography (TUG87) of the Canadian Rocky Mountains (m)

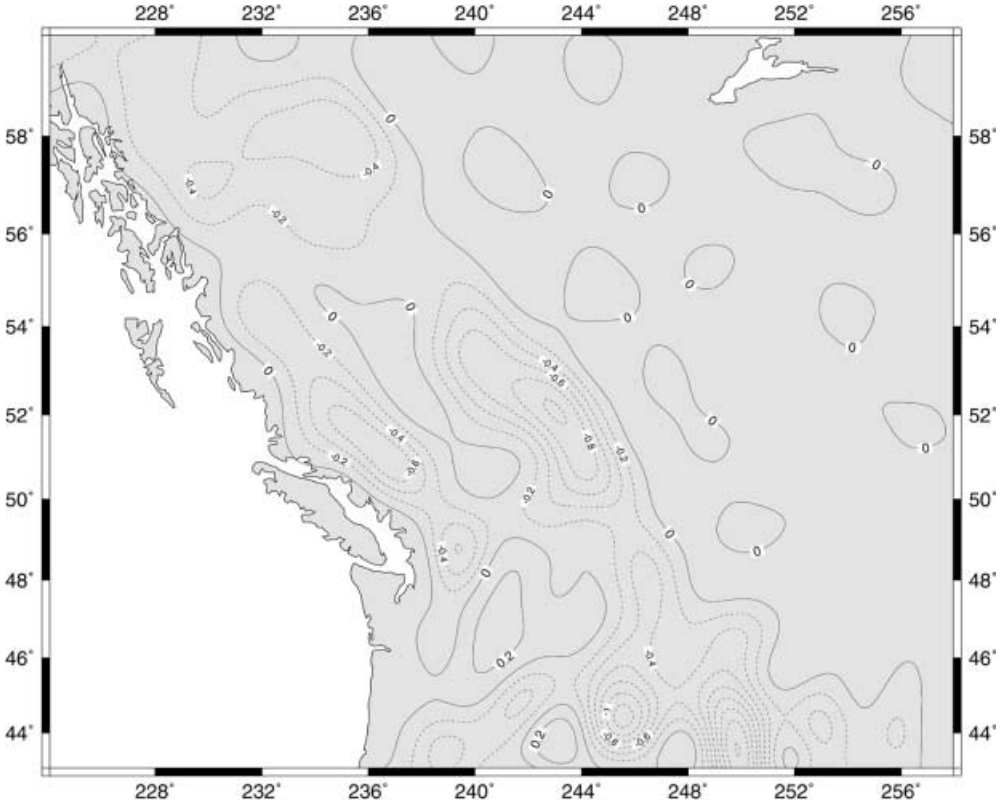

Fig. 2. Far-zone direct terrain effect on gravity D^{ter} (mGal)

were also discussed in Vaníček et al. (2001). We focus our attention on the difference $P^{\mathrm{ter}} = P^{\mathrm{t}} - P^{\mathrm{ct}}$, called in the following the 'primary indirect terrain effect' (PITerE). It is given by the following formula (Martinec and Vaníček 1994b):

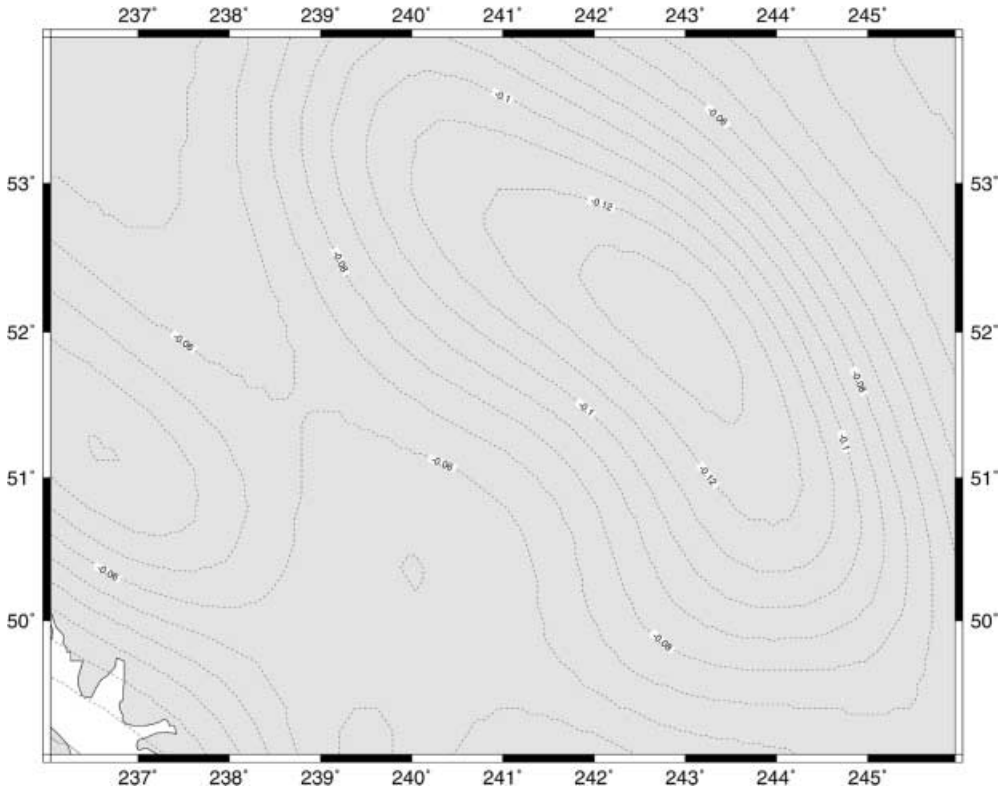

Fig. 3. Far-zone direct terrain effect on the geoid (m)

Table 1. Far-zone terrain effects on gravity (mGal)

Parameter	Minimum	Maximum	Mean value	Standard deviation
A^{t}	−43.993	+290.519	+55.599	±65.062
D^{ter}	−1.613	+0.351	−0.056	±0.220
S^{ter}	−0.266	+0.290	−0.005	±0.047

Table 2. Far-zone terrain effects on the geoid (m)

Parameter	Minimum	Maximum	Mean value	Standard deviation
A^{t}	+12.951	+50.682	+39.949	±6.681
D^{ter}	−0.136	+0.002	−0.073	±0.028
S^{ter}	−0.014	+0.011	−0.002	±0.006
P^{ter}	−0.295	+1.096	+0.053	±0.141

$$P^{\mathrm{ter}}(\Omega) = \frac{G}{\gamma}\varrho_{\mathrm{o}}^{\mathrm{t}} \iint_{\Omega_{\oplus}} \int_{\xi=R+H(\Omega)}^{R+H(\Omega')} \mathscr{L}^{-1}(R,\psi,\xi)\xi^2 \,\mathrm{d}\xi \,\mathrm{d}\Omega' - \frac{G}{\gamma}\varrho_{\mathrm{o}}^{\mathrm{t}} \iint_{\Omega_{\oplus}} \int_{\xi=R+H(\Omega)}^{R+H(\Omega')} \xi^2 \,\mathrm{d}\xi \mathscr{L}^{-1}(R,\psi,R) \,\mathrm{d}\Omega' \tag{17}$$

The near-zone contribution to the PITerE can also be computed by a 2-D numerical integration. The far-zone contribution to the PITerE can then be obtained again by the spectral approach. In order to obtain the far-zone contribution to the first integral in Eq. (17), the integration kernel

$$\int_{\xi=R+H(\Omega)}^{R+H(\Omega')} \mathscr{L}^{-1}(r,\psi,\xi)\xi^2 \,\mathrm{d}\xi \tag{18}$$

is developed into the spectral form (see Appendix B), which yields

$$2\pi\frac{G}{\gamma}\varrho_{\mathrm{o}}^{\mathrm{t}}\left[R\sum_{n=0}^{nh1} a_n(\eta,\psi,\psi_{\mathrm{o}})H_n(\Omega) + 2H(\Omega)\sum_{n=0}^{nh1} c_n(\eta,\psi,\psi_{\mathrm{o}})H_n(\Omega) + \sum_{n=0}^{nh2} b_n(\eta,\psi,\psi_{\mathrm{o}})H_n^2(\Omega) - \sum_{n=0}^{nh2} d_n(\eta,\psi,\psi_{\mathrm{o}})H_n^2(\Omega) + \mathscr{O}\left(\frac{H_n^3}{R}\right)\right] \tag{19}$$

Similarly, the Molodenskij spectral approach gives for the second integral in Eq. (17) the following series (see Appendix B):

$$2\pi\frac{G}{\gamma}\varrho_{\mathrm{o}}^{\mathrm{t}}\left[R\sum_{n=0}^{nh1} e_n(\psi,\psi_{\mathrm{o}})H_n(\Omega) + \sum_{n=0}^{nh2} e_n(\psi,\psi_{\mathrm{o}})H_n^2(\Omega) + \mathscr{O}\left(\frac{H_n^3}{R}\right)\right] \tag{20}$$

The Molodenskij truncation coefficients a_n, b_n, c_n, d_n and e_n are defined in Appendix B [see Eqs. (B14)–(B18)]. The far-zone primary indirect terrain effect is then the difference of the series defined by Eqs. (19) and (20)

$$
\begin{aligned}
&P^{\mathrm{ter}}(\Omega)\\
&\quad = 2\pi\frac{G}{\gamma}\varrho_{\mathrm{o}}^{\mathrm{t}}\Bigg[R\sum_{n=0}^{nh1}a_n(\eta,\psi,\psi_{\mathrm{o}})H_n(\Omega)+2H(\Omega)\\
&\qquad\times\sum_{n=0}^{nh1}c_n(\eta,\psi,\psi_{\mathrm{o}})H_n(\Omega)+\sum_{n=0}^{nh2}b_n(\eta,\psi,\psi_{\mathrm{o}})H_n^2(\Omega)\\
&\qquad-\sum_{n=0}^{nh2}d_n(\eta,\psi,\psi_{\mathrm{o}})H_n^2(\Omega)-R\sum_{n=0}^{nh1}e_n(\psi,\psi_{\mathrm{o}})H_n(\Omega)\\
&\qquad-\sum_{n=0}^{nh2}e_n(\psi,\psi_{\mathrm{o}})H_n^2(\Omega)+\mathcal{O}\left(\frac{H_n^3}{R}\right)\Bigg],\quad \forall\,\psi\geq\psi_{\mathrm{o}}>0
\end{aligned}
\tag{21}
$$

For our test area and the truncation radius $\psi_{\mathrm{o}}=3^{\circ}$, we obtain the numerical results shown in Fig. 4. The range of the values from Eq. (21), including basic statistical parameters such as the mean and the standard deviation, can be found in Table 2. It is interesting to note that, while the far-zone contribution to the DTerE on gravity is smaller than the near-zone contribution, the corresponding contributions to the PITerE are of comparable magnitude. This may originate in the fact that the potential is an inverse function of distance while gravity is an inverse function of distance squared and tapers off more quickly. Also, it should be noted that while the near-zone contribution is always negative, the far-zone contribution changes sign so that the resulting total PITE, although still predominantly negative, reaches positive values in some places. The far-zone contribution to the PITerE on the geoid is again of a long-wavelength character.

A spherical harmonic expression for the PITE on the geoid up to order H_n^3 was derived by Nahavandchi and Sjöberg [1998, Eq. (24)], which is also intended for the computation of the global PITE using the full spatial angle $\Omega_{\oplus}$. A new formula, compromising between the local integration and the spherical harmonic expression, was derived in Sjöberg and Nahavandchi [1998, Eq. (12)].

5 The secondary indirect topographical effect on gravity

For the Stokes–Helmert problem, the spherical form of the SITE on gravity was formulated in Vaníček et al. (1999) as a re-scaled value (the scale is equal to $2/R$) of the residual topographical potential evaluated at radius $R+H$; see Eq. (5). Since the difference of the gravitational potential of the spherical topographical shell and its condensed counterpart is for the mass conservation condensation equal to zero, the so-called secondary indirect terrain effect SITerE accounts for the entire SITE on gravity. The SITerE on gravity (S^{ter}) can be computed by the following expression (Vaníček et al. 1999):

$$
\begin{aligned}
&S^{\mathrm{ter}}(R+H,\Omega)\\
&\quad=\frac{2G}{R}\varrho_{\mathrm{o}}^{\mathrm{t}}\iint_{\Omega_{\oplus}}\int_{\xi=R+H(\Omega)}^{R+H(\Omega')}\mathscr{L}^{-1}(R+H,\psi,\xi)\xi^2\,\mathrm{d}\xi\,\mathrm{d}\Omega'\\
&\qquad-\frac{2G}{R}\varrho_{\mathrm{o}}^{\mathrm{t}}\iint_{\Omega_{\oplus}}\mathscr{L}^{-1}(R+H,\psi,R)\int_{\xi=R+H(\Omega)}^{R+H(\Omega')}\xi^2\,\mathrm{d}\xi\,\mathrm{d}\Omega'
\end{aligned}
\tag{22}
$$

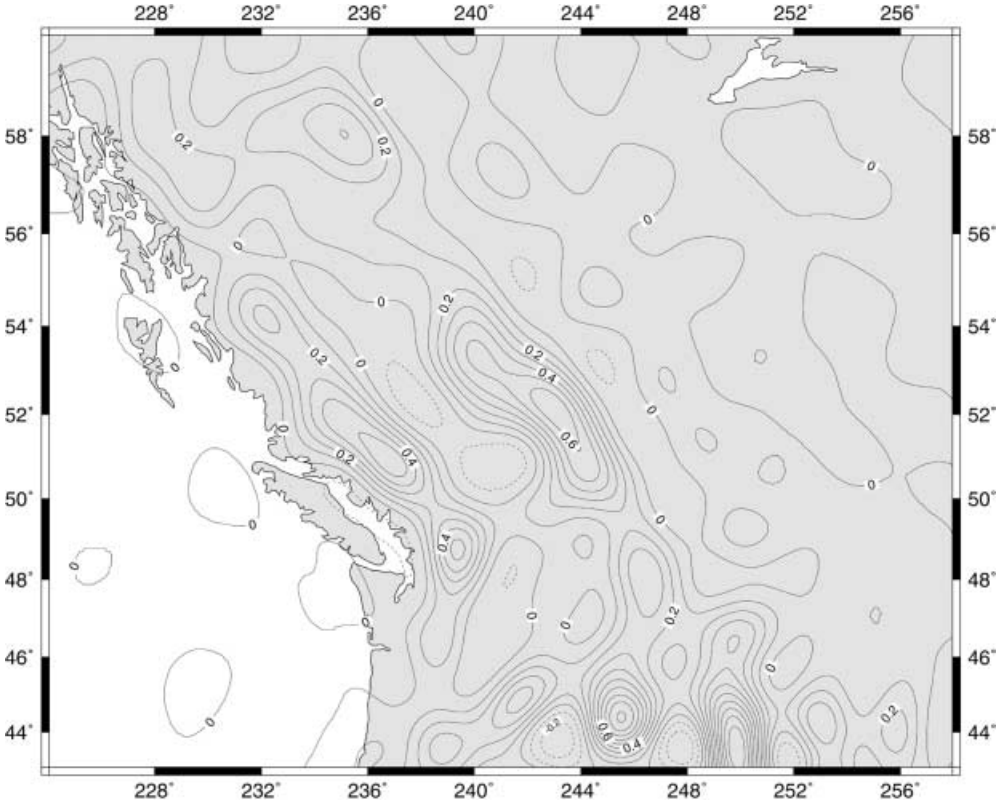

Fig. 4. Far-zone primary indirect terrain effect on the geoid P^{ter} (m)

The near-zone effect can be computed by a standard 2-D numerical integration discretizing the corresponding formulae by the Gaussian quadrature rule. To compute its far-zone contribution, the integration kernel of the first integral in Eq. (22), i.e.

$$\int_{\xi=R+H(\Omega)}^{R+H(\Omega')} \mathscr{L}^{-1}(R+H,\psi,\xi)\xi^2\,\mathrm{d}\xi \tag{23}$$

can be transformed into the spectral form (see Appendix C), which gives

$$4\pi G\varrho_{\mathrm{o}}^{\mathrm{t}}\left[\frac{R+H(\Omega)}{R}\sum_{n=0}^{nh1}p_n(\psi,\psi_{\mathrm{o}})H_n(\Omega) - 2\frac{H(\Omega)}{R}\sum_{n=0}^{nh1}q_n(\psi,\psi_{\mathrm{o}})H_n(\Omega) + \frac{1}{R}\sum_{n=0}^{nh2}r_n(\psi,\psi_{\mathrm{o}})H_n^2(\Omega) + \mathscr{O}\left(\frac{H_n^3}{R^2}\right)\right] \tag{24}$$

Similarly, the second integral in Eq. (22) can be developed into (see Appendix C)

$$4\pi G\varrho_{\mathrm{o}}^{\mathrm{t}}\left[\sum_{n=0}^{nh1}s_n(H,\psi,\psi_{\mathrm{o}})H_n(\Omega) + \frac{1}{R}\sum_{n=0}^{nh2}s_n(H,\psi,\psi_{\mathrm{o}})H_n^2(\Omega) + \mathscr{O}\left(\frac{H_n^3}{R^2}\right)\right] \tag{25}$$

The Molodenskij truncation coefficients p_n, q_n, r_n and s_n are also defined in Appendix C [see Eqs. (C9)–(C12)]. Subtracting the series of Eqs. (24) and (25), the far-zone contribution to the SITerE on gravity reads

$$\begin{aligned} S^{\mathrm{ter}}(R+H,\Omega) &= 4\pi G\varrho_{\mathrm{o}}^{\mathrm{t}}\left[\frac{R+H(\Omega)}{R}\sum_{n=0}^{nh1}p_n(\psi,\psi_{\mathrm{o}})H_n(\Omega)\right. \\ &\quad - 2\frac{H(\Omega)}{R}\sum_{n=0}^{nh1}q_n(\psi,\psi_{\mathrm{o}})H_n(\Omega) + \frac{1}{R}\sum_{n=0}^{nh2}r_n(\psi,\psi_{\mathrm{o}})H_n^2(\Omega) \\ &\quad - \sum_{n=0}^{nh1}s_n(H,\psi,\psi_{\mathrm{o}})H_n(\Omega) - \frac{1}{R}\sum_{n=0}^{nh2}s_n(H,\psi,\psi_{\mathrm{o}})H_n^2(\Omega) \\ &\quad \left.+ \mathscr{O}\left(\frac{H_n^3}{R^2}\right)\right], \quad \forall\,\psi \geq \psi_{\mathrm{o}} > 0 \end{aligned} \tag{26}$$

The far-zone SITerE on gravity S^{ter}, computed by Eq. (26) over the test area using the truncation radius of $\psi_{\mathrm{o}} = 3^\circ$, is shown in Fig. 5. Corresponding effects on the geoid, obtained by continuing these values down to the geoid and applying Stokes' integration, are shown in Fig. 6. The extreme values for the SITerE on gravity can be found in Tables 1 and 2, including their basic statistical parameters. The near and far-zone contributions to the SITerE are also of comparable magnitude. The same argument as in the case of the PITerE could be used here. The values of the SITerE are at the accuracy level required in current geoid computations and should still be taken into the account. The far-zone contribution to the SITerE on gravity is also of a long-wavelength character.

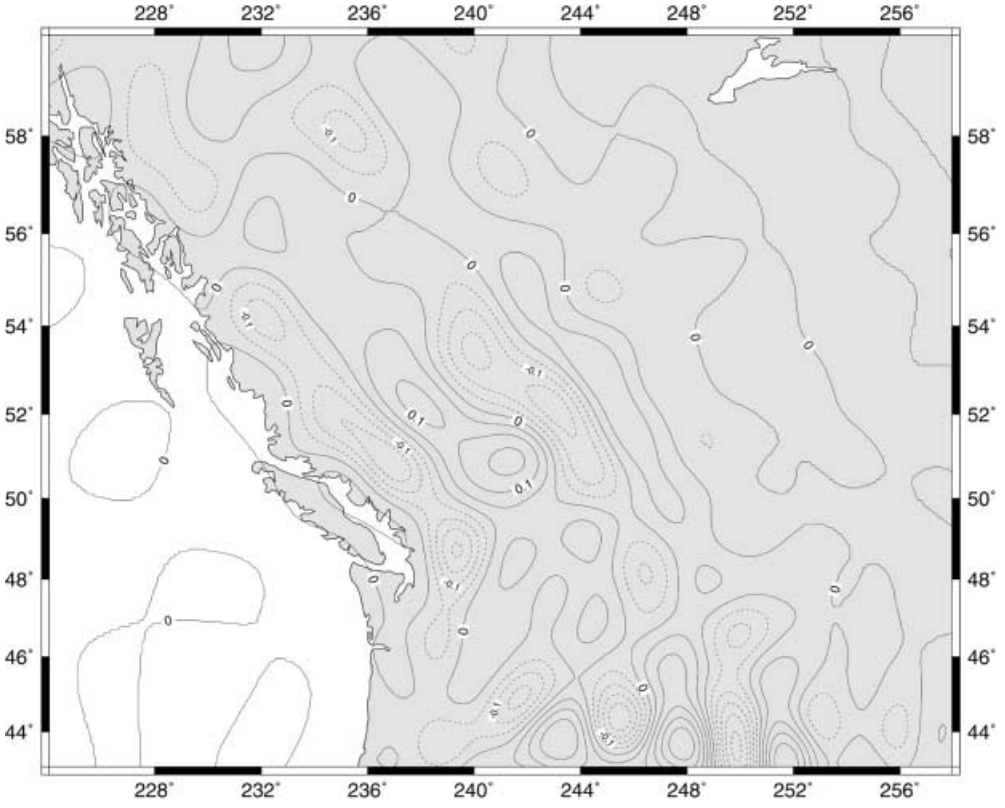

Fig. 5. Far-zone secondary indirect terrain effect on gravity S^{ter} (mGal)

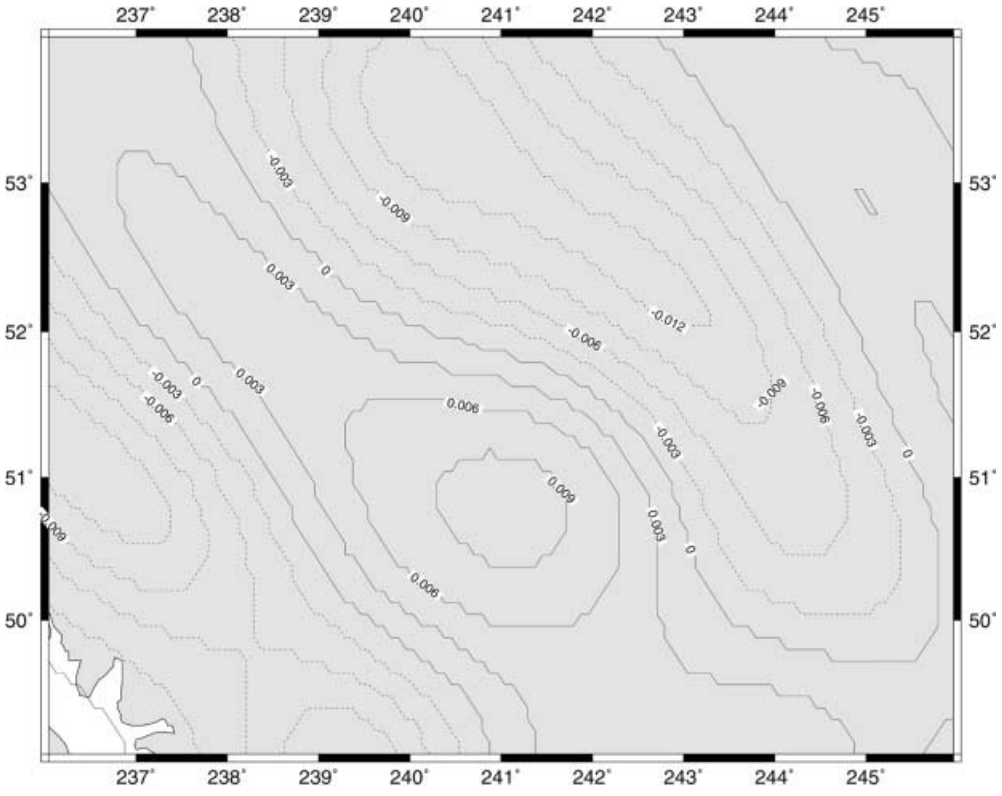

Fig. 6. Far-zone secondary indirect terrain effect on the geoid (m)

A comparable spherical harmonic expression for the SITE on gravity up to order H_n^3 was again derived by Nahavandchi and Sjöberg [1998, Eq. (25)].

6 The terrain correction

Clearly, Eq. (11) by itself describes the terrain correction to gravity used in the evaluation of the refined Bouguer anomaly and the Fay anomaly (Heiskanen and Moritz 1967). It is thus also worth looking at it alone – in addition to looking at the difference of Eqs. (11) and (12). Figure 7 shows the values of the far-zone contribution to the terrain correction A^{t} for our test area. It is very large and again of a long-wavelength character.

It is of interest to compare the spherical terrain correction with the standard planar terrain correction used in practice. Figure 8 shows the difference between the standard planar terrain correction (TC), and our terrain correction computed from a spherical model taking into account the topography from all around the world. The differences are very significant, but they are predominantly of a long-wavelength nature. They thus do not affect the routine geophysical interpretation of the Bouguer gravity anomalies, which seeks shallow density anomalies. If deeper-seeded anomalies are of interest, the spherical terrain correction must be considered.

7 Conclusions

In this contribution, the far-zone spherical terrain effects both on gravity and the geoid, which originate in the second Helmert condensation of external topographical masses, were discussed. These effects are usually deemed to be too small, and thus often neglected in practical geoid computations. As a consequence of this belief, the planar approximation of the terrain is usually deployed for the evaluation of the terrain effects on gravity and the geoid. Based on the numerical values obtained in our computations, we believe that the planar approximation is not adequate and its use can be responsible for the long-wavelength errors in the geoid solutions. They can be directly transformed into the geoidal undulations through the low-pass filtering in the Stokes integration. For comparable conclusions see, for example, Sjöberg and Nahavandchi (1998) and Nahavandchi (2000).

The far-zone spherical terrain effects, due to their large magnitude, are very important for the evaluation of the centimetre geoid. The direct and the primary indirect terrain effects have the most significant contribution to the geoid. The far-zone direct terrain effect can easily reach values on the decimetre level (see Table 2). The far-zone primary indirect terrain effect has the largest contribution on the metre level but its average magnitude is significantly smaller (again see Table 2). The far-zone secondary indirect terrain effect, although the smallest of all the terrain effects, should still be taken into the account for the evaluation of the centimetre geoid although its magnitude is the smallest of all the far-terrain effects we introduced in this contribution.

An important finding is represented by the values of the far-zone spherical terrain correction. For applications where the compensation is not required (such as the derivation of the refined Bouguer anomalies in geophysical applications), the difference between the planar and the

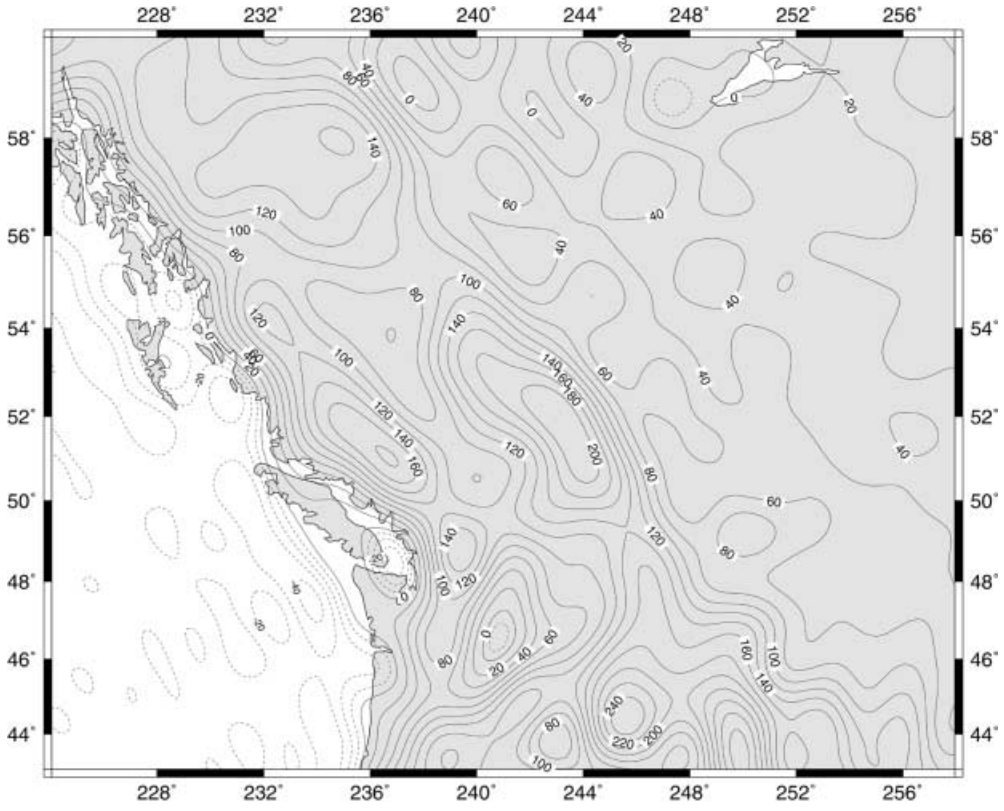

Fig. 7. Far-zone terrain correction to gravity A^t (mGal)

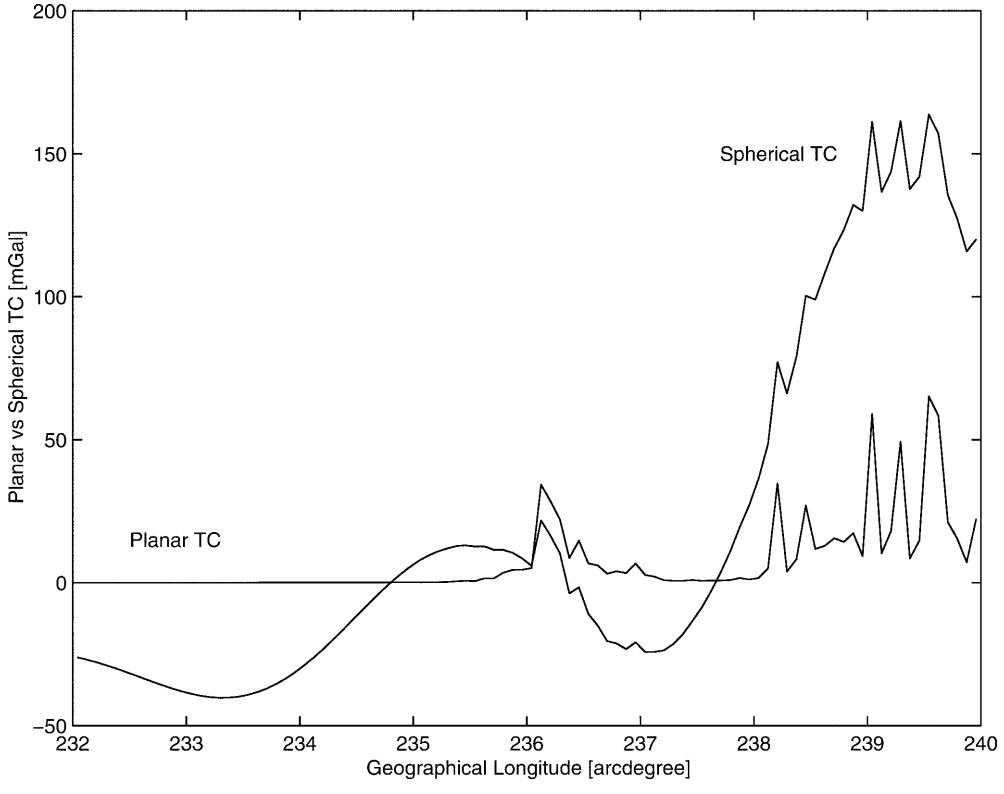

Fig. 8. Spherical vs planar terrain correction to gravity (mGal)

spherical model can be very significant (see Fig. 8). In Fig. 8, the total terrain correction to gravity along the selected parallel across the Coastal Mountains in western Canada, computed using the planar and the spherical terrain model, is shown. It is the far-zone effect (clearly missing in the planar model) which distinguishes the planar and the spherical values. Therefore we should keep in mind the fact that the use of the planar and the spherical model of the topography may have serious consequences if applied in specific applications.

The topographical effects are the most important corrections to both gravity and the geoid. They represent, together with accuracy and density of observed gravity data, one of the most serious limits on higher accuracy of the gravimetric geoid today. Their correct evaluation depends on the correct knowledge of input data (topographical heights and the mass density of the topography), and sufficiently accurate modelling of the topographical masses. The knowledge of the global topography will greatly improve in the near future due to the latest Shuttle Radar Topography Mission, which used an advanced radar technique to obtain data for production of the most precise, near-global topographical map ever (nearly 80% of the Earth's landmass), and which will leave us with the incomplete knowledge of the topographical mass density distribution as the major problem in the topographical reduction of gravity data. The formulation of the terrain effects based on the spherical rather than the planar approximation, which allows us to account for the low-frequency effects of the far-zone terrain on both gravity and the geoid, represents then the major contribution of the presented research. When combined with the corresponding high-frequency effects computed by a 2-D integration over the near-zone terrain, proper values of topographical effects can be obtained.

Appendix A

Truncation coefficients for DTerE

In this appendix, the truncation coefficients for the direct terrain effect on gravity are derived. The integration kernel of Eq. (10) is developed in its general form as follows (Gradshteyn and Ryzhik 1980):

$$\begin{aligned}\frac{\partial}{\partial r}\int_{\xi}\mathscr{L}^{-1}(r,\psi,\xi)\xi^2\,\mathrm{d}\xi\Big|_r &= \left[(\xi^2+3r^2)\cos\psi + r\xi(1-6\cos^2\psi)\right]\mathscr{L}^{-1}(r,\psi,\xi)\\ &\quad + r(3\cos^2\psi-1)\ln|\xi - r\cos\psi + \mathscr{L}(r,\psi,\xi)| \end{aligned}\tag{A1}$$

The Newtonian kernel $\mathscr{L}^{-1}$ [see Eq. (8)] can be developed into a binomial series

$$\begin{aligned}&\mathscr{L}^{-1}(r,\psi,\xi)\\ &\quad = \frac{1}{r}(2-2\cos\psi)^{-\frac{1}{2}}\left[1+\zeta\left(1+\frac{\zeta}{2-2\cos\psi}\right)\right]^{-\frac{1}{2}}\\ &\quad = \frac{1}{r}(2-2\cos\psi)^{-\frac{1}{2}}\left(1-\frac{\zeta}{2}+\frac{\zeta^2}{8}\frac{1-3\cos\psi}{1-\cos\psi}\right)+\mathscr{O}(\zeta^3)\end{aligned}\tag{A2}$$

where the following substitution is used:

$$\eta=\frac{\xi}{r}=1+\zeta,\quad \text{i.e. } \zeta=\frac{\xi}{r}-1\tag{A3}$$

The parameter r is equal to $R+H(\Omega)$, and the parameter ξ is equal either to $R+H(\Omega)$ or to $R+H(\Omega')$. The truncation of the binomial series in Eq. (A2) after the quadratic term is fully justified for the range of values of ψ and ζ used in our computations, i.e. for $\psi\geq\psi_o=3^\circ$, and for $|\zeta|<0.0015$ (for maximum topographical height of 9 km), which yield

$$\left|\zeta\left(1+\frac{\zeta}{2-2\cos\psi}\right)\right|<0.0025\ll 1\tag{A4}$$

Similarly, the inverse of the Newtonian kernel, i.e. $\mathscr{L}$, can be developed as follows:

$$\mathscr{L}(r,\psi,\xi)=r(2-2\cos\psi)^{\frac{1}{2}}\left(1+\frac{\zeta}{2}+\frac{\zeta^2}{8}\frac{1+\cos\psi}{1-\cos\psi}\right)+\mathscr{O}(\zeta^3)\tag{A5}$$

Using the substitutions of Eqs. (A2) and (A5), the integration kernel of Eq. (A1) can be written as follows:

$$\begin{aligned}&r\frac{(3+\eta^2)\cos\psi+\eta(1-6\cos^2\psi)}{(1+\eta^2-2\eta\cos\psi)^{\frac{1}{2}}}-r\frac{1+4\cos\psi-6\cos^2\psi}{(2-2\cos\psi)^{\frac{1}{2}}}\\ &\quad + r(3\cos^2\psi-1)\ln\left|\frac{\eta-\cos\psi+(1+\eta^2-2\eta\cos\psi)^{\frac{1}{2}}}{1-\cos\psi+(2-2\cos\psi)^{\frac{1}{2}}}\right|\end{aligned}\tag{A6}$$

The logarithmic function in Eq. (A6) can further be expanded into the Taylor series which, following the above reasoning can also be truncated after the quadratic term

$$\begin{aligned}&\ln\left|\frac{\eta-\cos\psi+(1+\eta^2-2\eta\cos\psi)^{\frac{1}{2}}}{1-\cos\psi+(2-2\cos\psi)^{\frac{1}{2}}}\right|\\ &\quad=\frac{\zeta+(2-2\cos\psi)^{\frac{1}{2}}\left(\frac{\zeta}{2}+\frac{\zeta^2}{8}\frac{1+\cos\psi}{1-\cos\psi}\right)}{1-\cos\psi+(2-2\cos\psi)^{\frac{1}{2}}}\\ &\qquad-\frac{1}{2}\left[\frac{\zeta+(2-2\cos\psi)^{\frac{1}{2}}\left(\frac{\zeta}{2}+\frac{\zeta^2}{8}\frac{1+\cos\psi}{1-\cos\psi}\right)}{1-\cos\psi+(2-2\cos\psi)^{\frac{1}{2}}}\right]^2+\mathscr{O}(\zeta^3)\end{aligned}\tag{A7}$$

Substituting the expression in Eq. (A7) into Eq. (A6), the integration kernel of Eq. (A1) can subsequently be developed into the form

$$\begin{aligned}\frac{\partial}{\partial r}\int_{\xi}\mathscr{L}^{-1}(r,\psi,\xi)\xi^2\,\mathrm{d}\xi\Big|_r &= -\frac{r}{2}\zeta(2-2\cos\psi)^{-\frac{1}{2}}-\frac{r}{8}\zeta^2\\ &\quad\times\frac{3-10\cos\psi+3\cos^2\psi-2(3\cos\psi-1)(2-2\cos\psi)^{\frac{1}{2}}}{(2-2\cos\psi)^{\frac{1}{2}}\left[1-\cos\psi+(2-2\cos\psi)^{\frac{1}{2}}\right]^2}\\ &\quad+\mathscr{O}(\zeta^3)\end{aligned}\tag{A8}$$

which, after substitutions for the actual integration limits, i.e. $\xi = R + H(\Omega)$ and $\xi = R + H(\Omega')$, can be written as follows:

$$\frac{\partial}{\partial r}\int_{\xi=R+H(\Omega)}^{R+H(\Omega')} \mathscr{L}^{-1}(r,\psi,\xi)\xi^2\,\mathrm{d}\xi\Big|_{r=R+H(\Omega)} = [H(\Omega') - H(\Omega)]\mathscr{K}_1(\psi) + \frac{1}{R+H(\Omega)} \times [H(\Omega') - H(\Omega)]^2\mathscr{K}_2(\psi) + \mathscr{O}\left[\frac{H^3}{(R+H)^2}\right] \quad \text{(A9)}$$

The integration kernel $\mathscr{K}_1$ in Eq. (A9) is of the following form:

$$\mathscr{K}_1(\psi) = -\frac{1}{4}\frac{(2-2\cos\psi)^{\frac{1}{2}}}{1-\cos\psi} \quad \text{(A10)}$$

and the integration kernel $\mathscr{K}_2$ reads

$$\mathscr{K}_2(\psi) = -\frac{1}{8}\frac{3-10\cos\psi+3\cos^2\psi-2(3\cos\psi-1)(2-2\cos\psi)^{\frac{1}{2}}}{(2-2\cos\psi)^{\frac{1}{2}}\left[1-\cos\psi+(2-2\cos\psi)^{\frac{1}{2}}\right]^2} \quad \text{(A11)}$$

The integration kernel of the second integral in Eq. (7) can simply be written

$$\int_{\xi=R+H(\Omega)}^{R+H(\Omega')} \xi^2\,\mathrm{d}\xi\frac{\partial}{\partial r}\mathscr{L}^{-1}(r,\psi,R)\Big|_{r=R+H(\Omega)} = R^2\left[H(\Omega') - H(\Omega) + \frac{H^2(\Omega') - H^2(\Omega)}{R}\right] \times \mathscr{J}(R,\psi,R+H) + \mathscr{O}\left[\frac{H^3}{R^2}\right] \quad \text{(A12)}$$

with the function $\mathscr{J}$ defined as the radial derivative of the Newtonian kernel $\mathscr{L}^{-1}$ (Heiskanen and Moritz 1967, Sect. 1.16)

$$\mathscr{J}(R,\psi,R+H) = \frac{R(\cos\psi-1)-H}{\mathscr{L}^3(R,\psi,R+H)} \quad \text{(A13)}$$

The truncation coefficients, used in Eqs. (11) and (12), can finally be estimated by the 1-D integration over the spherical distance ψ

$$t_n(\psi,\psi_o) = \int_{\psi=\psi_o}^{\pi} \mathscr{K}_1(\psi)[P_n(\cos\psi)-1]\sin\psi\,\mathrm{d}\psi, \quad \forall n = 0,\ldots,nh1 \quad \text{(A14)}$$

$$u_n(\psi,\psi_o) = \int_{\psi=\psi_o}^{\pi} \mathscr{K}_2(\psi)P_n(\cos\psi)\sin\psi\,\mathrm{d}\psi, \quad \forall n = 0,\ldots,nh1 \quad \text{(A15)}$$

$$v_n(\psi,\psi_o) = \int_{\psi=\psi_o}^{\pi} \mathscr{K}_2(\psi)[P_n(\cos\psi)+1]\sin\psi\,\mathrm{d}\psi, \quad \forall n = 0,\ldots,nh2 \quad \text{(A16)}$$

$$w_n(H,\psi,\psi_o) = R^2\int_{\psi=\psi_o}^{\pi} \mathscr{J}(R,\psi,R+H)[P_n(\cos\psi)-1]\sin\psi\,\mathrm{d}\psi, \quad \forall n \geq 0 \quad \text{(A17)}$$

Appendix B

Truncation coefficients for PITerE

In this appendix, the truncation coefficients for the primary indirect terrain effect on the geoid are derived. The integration kernel of Eq. (18) can be derived as a primitive function of the Newtonian kernel $\mathscr{L}^{-1}$ (Gradshteyn and Ryzhik 1980)

$$\int_{\xi} \mathscr{L}^{-1}(r,\psi,\xi)\xi^2\,\mathrm{d}\xi = \frac{1}{2}(\xi+3r\cos\psi)\mathscr{L}(r,\psi,\xi) + \frac{r^2}{2}(3\cos^2\psi-1)\,\ln|\xi - r\cos\psi + \mathscr{L}(r,\psi,\xi)| + C \quad \text{(B1)}$$

where C stands for the integration constant. Introducing the following two unitless parameters:

$$\eta = \frac{R+H(\Omega)}{R} = 1+\zeta \quad \text{(B2)}$$

$$\eta' = \frac{R+H(\Omega')}{R} = 1+\zeta' \quad \text{(B3)}$$

and using the substitutions from the previous section, we obtain

$$\int_{\xi=R+H(\Omega)}^{R+H(\Omega')} \mathscr{L}^{-1}(r,\psi,\xi)\xi^2\,\mathrm{d}\xi = \frac{R^2}{2}(\eta'+3\cos\psi)(1+\eta'^2-2\eta'\cos\psi)^{\frac{1}{2}} + \frac{R^2}{2}(3\cos^2\psi-1)\ln\left|\frac{\eta'-\cos\psi+(1+\eta'^2-2\eta'\cos\psi)^{\frac{1}{2}}}{\eta-\cos\psi+(1+\eta^2-2\eta\cos\psi)^{\frac{1}{2}}}\right| - \frac{R^2}{2}(\eta+3\cos\psi)(1+\eta^2-2\eta\cos\psi)^{\frac{1}{2}} \quad \text{(B4)}$$

The first and third expressions on the right-hand side of Eq. (B4) can be developed using

$$(\eta' + 3\cos\psi)(1 + \eta'^2 - 2\,\eta'\cos\psi)^{\frac{1}{2}} \sim (1 + \zeta' + 3\cos\psi)(2 - 2\cos\psi)^{\frac{1}{2}} \times \left(1 + \frac{\zeta'}{2} + \frac{\zeta'^2}{8}\frac{1+\cos\psi}{1-\cos\psi}\right) + \mathcal{O}(\zeta'^3) \tag{B5}$$

$$(\eta + 3\cos\psi)(1 + \eta^2 - 2\eta\cos\psi)^{\frac{1}{2}} \sim (1 + \zeta + 3\cos\psi)(2 - 2\cos\psi)^{\frac{1}{2}} \times \left(1 + \frac{\zeta}{2} + \frac{\zeta^2}{8}\frac{1+\cos\psi}{1-\cos\psi}\right) + \mathcal{O}(\zeta^3) \tag{B6}$$

and the logarithmic function can be expanded as follows [cf. Eq. (A7)]

$$\ln\left|\frac{\eta' - \cos\psi + (1 + \eta'^2 - 2\eta'\cos\psi)^{\frac{1}{2}}}{\eta - \cos\psi + (1 + \eta^2 - 2\eta\cos\psi)^{\frac{1}{2}}}\right| = \frac{\zeta' - \zeta + (2 - 2\cos\psi)^{\frac{1}{2}}\left(\frac{\zeta'-\zeta}{2} + \frac{\zeta'^2-\zeta^2}{8}\frac{1+\cos\psi}{1-\cos\psi}\right)}{\eta - \cos\psi + (1 + \eta^2 - 2\eta\cos\psi)^{\frac{1}{2}}} - \frac{1}{2}\left[\frac{\zeta' - \zeta + (2 - 2\cos\psi)^{\frac{1}{2}}\left(\frac{\zeta'-\zeta}{2} + \frac{\zeta'^2-\zeta^2}{8}\frac{1+\cos\psi}{1-\cos\psi}\right)}{\eta - \cos\psi + (1 + \eta^2 - 2\eta\cos\psi)^{\frac{1}{2}}}\right]^2 + \mathcal{O}(\zeta^3) \tag{B7}$$

The expressions in Eqs. (B5)–(B7) can be further simplified using elementary algebraic operations. Their substitution into Eq. (B4) yields the integration kernel of Eq. (B1) in the following form:

$$\begin{aligned}\int_{\xi=R+H(\Omega)}^{R+H(\Omega')} \mathscr{L}^{-1}(r,\psi,\xi)\xi^2\,\mathrm{d}\xi &= \frac{3R^2}{4}(\zeta' - \zeta)(2 - 2\cos\psi)^{\frac{1}{2}}(1 + \cos\psi) + \frac{R^2}{8}(\zeta'^2 - \zeta^2) \\ &\times \frac{(3\cos^2\psi - 1)(1 + \cos\psi)}{(2 - 2\cos\psi)^{\frac{1}{2}}\left[\eta - \cos\psi + (1 + \eta^2 - 2\eta\cos\psi)^{\frac{1}{2}}\right]} \\ &- \frac{R^2}{8}(\zeta' - \zeta)^2(3\cos^2\psi - 1) \\ &\times \frac{3 - \cos\psi + 2(2 - 2\cos\psi)^{\frac{1}{2}}}{\left[\eta - \cos\psi + (1 + \eta^2 - 2\eta\cos\psi)^{\frac{1}{2}}\right]^2} \\ &+ \frac{R^2}{4}(\zeta' - \zeta)(3\cos^2\psi - 1) \\ &\times \frac{2 + (2 - 2\cos\psi)^{\frac{1}{2}}}{\eta - \cos\psi + (1 + \eta^2 - 2\eta\cos\psi)^{\frac{1}{2}}} \\ &+ \frac{R^2}{8}(\zeta'^2 - \zeta^2)\frac{5 + 3\cos^2\psi}{(2 - 2\cos\psi)^{\frac{1}{2}}} + \mathcal{O}(\zeta^3)\end{aligned} \tag{B8}$$

Substituting for the actual integration limits, Eq. (B8) can be developed into the following form which can be used for practical computations:

$$\begin{aligned}\int_{\xi=R+H(\Omega)}^{R+H(\Omega')} \mathscr{L}^{-1}(r,\psi,\xi)\xi^2\,\mathrm{d}\xi &= R[H(\Omega') - H(\Omega)]\mathscr{H}_1(\eta,\psi) \\ &+ \left[H^2(\Omega') - H^2(\Omega)\right]\mathscr{H}_2(\eta,\psi) \\ &- [H(\Omega') - H(\Omega)]^2\mathscr{H}_3(\eta,\psi) + \mathcal{O}\left[\frac{H^3}{R}\right]\end{aligned} \tag{B9}$$

where the integration kernels read

$$\mathscr{H}_1(\eta,\psi) = \frac{3}{4}(2 - 2\cos\psi)^{\frac{1}{2}}(1 + \cos\psi) + \frac{(3\cos^2\psi - 1)\left[2 + (2 - 2\cos\psi)^{\frac{1}{2}}\right]}{4\left[\eta - \cos\psi + (1 + \eta^2 - 2\eta\cos\psi)^{\frac{1}{2}}\right]} \tag{B10}$$

$$\mathscr{H}_2(\eta,\psi) = \frac{5 + 3\cos^2\psi}{8(2 - 2\cos\psi)^{\frac{1}{2}}} + \frac{(3\cos^2\psi - 1)(1 + \cos\psi)}{8(2 - 2\cos\psi)^{\frac{1}{2}}\left[\eta - \cos\psi + (1 + \eta^2 - 2\eta\cos\psi)^{\frac{1}{2}}\right]} \tag{B11}$$

$$\mathscr{H}_3(\eta,\psi) = \frac{(3\cos^2\psi - 1)\left[3 - \cos\psi + 2(2 - 2\cos\psi)^{\frac{1}{2}}\right]}{8\left[\eta - \cos\psi + (1 + \eta^2 - 2\eta\cos\psi)^{\frac{1}{2}}\right]^2} \tag{B12}$$

The integration kernel of the second integral in Eq. (17) is simply developed into another series truncated after the quadratic term

$$\begin{aligned}\mathscr{L}^{-1}(R,\psi,R)\int_{\xi=R+H(\Omega)}^{R+H(\Omega')} \xi^2\,\mathrm{d}\xi &= R^2\left[H(\Omega') - H(\Omega) + \frac{H^2(\Omega') - H^2(\Omega)}{R}\right] \\ &\times \mathscr{L}^{-1}(R,\psi,R) + \mathcal{O}\left[\frac{H^3}{R}\right]\end{aligned} \tag{B13}$$

Finally, the truncation coefficients in Eqs. (19) and (20) can again be evaluated by the 1-D integration over the spherical distance ψ

$$a_n(\eta,\psi,\psi_o) = \int_{\psi=\psi_o}^{\pi} \mathscr{H}_1(\eta,\psi)[P_n(\cos\psi) - 1]\sin\psi\,\mathrm{d}\psi, \quad \forall\, n = 0,\ldots,nh1 \tag{B14}$$

$$b_n(\eta,\psi,\psi_o) = \int_{\psi=\psi_o}^{\pi} \mathscr{H}_2(\eta,\psi)[P_n(\cos\psi)-1]\sin\psi\,\mathrm{d}\psi, \quad \forall n = 0,\ldots,nh2 \tag{B15}$$

$$c_n(\eta,\psi,\psi_o) = \int_{\psi=\psi_o}^{\pi} \mathscr{H}_3(\eta,\psi)P_n(\cos\psi)\sin\psi\,\mathrm{d}\psi, \quad \forall n = 0,\ldots,nh1 \tag{B16}$$

$$d_n(\eta,\psi,\psi_o) = \int_{\psi=\psi_o}^{\pi} \mathscr{H}_3(\eta,\psi)[P_n(\cos\psi)+1]\sin\psi\,\mathrm{d}\psi, \quad \forall n = 0,\ldots,nh2 \tag{B17}$$

$$e_n(\psi,\psi_o) = R\int_{\psi=\psi_o}^{\pi} \mathscr{L}^{-1}(R,\psi,R)[P_n(\cos\psi)-1]\sin\psi\,\mathrm{d}\psi, \quad \forall n \geq 0 \tag{B18}$$

The parameter η is equal to

$$\eta = 1 + \frac{H(\Omega)}{R} \tag{B19}$$

In practice, the coefficients of Eqs. (B14)–(B18) are evaluated in the form of tables for the selected reference heights. During computations, the heights of computation points are used to find the appropriate kernel values using some of available interpolation techniques (e.g. Lagrange's interpolation).

Appendix C

Truncation coefficients for SITerE

Let the parameter η now be defined as follows:

$$\eta = \frac{R+H(\Omega')}{R+H(\Omega)} = \frac{R+H'}{R+H} = \frac{r'}{r} \tag{C1}$$

and the parameter ζ as

$$\zeta = \frac{r'-r}{r} = \frac{H'-H}{R+H} = \eta - 1 \tag{C2}$$

The integration kernel of Eq. (23) can be formulated for the specified integration limits as

$$\begin{aligned}\int_{\xi=R+H(\Omega)}^{R+H(\Omega')} \mathscr{L}^{-1}(r,\psi,\xi)\xi^2\,\mathrm{d}\xi &= \frac{r^2}{2}(\eta+3\cos\psi)(1+\eta^2-2\eta\cos\psi)^{\frac{1}{2}} + \frac{r^2}{2}(3\cos^2\psi-1)\\ &\quad\times\ln\left|\frac{\eta-\cos\psi+(1+\eta^2-2\eta\cos\psi)^{\frac{1}{2}}}{1-\cos\psi+(2-2\cos\psi)^{\frac{1}{2}}}\right|\\ &\quad-\frac{r^2}{2}(1+3\cos\psi)(2-2\cos\psi)^{\frac{1}{2}}\end{aligned} \tag{C3}$$

Deploying the power series expansion of the logarithmic function, cf. Eq. (A7), and performing all algebraic operations, we obtain

$$\begin{aligned}\int_{\xi=R+H(\Omega)}^{R+H(\Omega')} \mathscr{L}^{-1}(r,\psi,\xi)\xi^2\,\mathrm{d}\xi &= \frac{r^2}{2}\zeta\frac{2+(2-2\cos\psi)^{\frac{1}{2}}}{1-\cos\psi+(2-2\cos\psi)^{\frac{1}{2}}} + \frac{3r^2}{4}\zeta^2\\ &\quad\times\frac{3-4\cos\psi+\cos^2\psi+2(1-\cos\psi)(2-2\cos\psi)^{\frac{1}{2}}}{(2-2\cos\psi)^{\frac{1}{2}}\left[1-\cos\psi+(2-2\cos\psi)^{\frac{1}{2}}\right]^2}\\ &\quad+\mathscr{O}(\zeta^3)\end{aligned} \tag{C4}$$

After substitutions for the actual integration limits, Eq. (C4) can be developed into the following form:

$$\begin{aligned}\int_{\xi=R+H(\Omega)}^{R+H(\Omega')} \mathscr{L}^{-1}(R+H,\psi,\xi)\xi^2\,\mathrm{d}\xi &= [H(\Omega')-H(\Omega)][R+H(\Omega)]\mathscr{M}_1(\psi)\,\mathrm{d}\Omega'\\ &\quad+[H(\Omega')-H(\Omega)]^2\mathscr{M}_2(\psi)\,\mathrm{d}\Omega'+\mathscr{O}\left[\frac{H^3}{R+H}\right]\end{aligned} \tag{C5}$$

where the corresponding integration kernels are

$$\mathscr{M}_1(\psi) = \frac{2+(2-2\cos\psi)^{\frac{1}{2}}}{2\left[1-\cos\psi+(2-2\cos\psi)^{\frac{1}{2}}\right]} \tag{C6}$$

$$\mathscr{M}_2(\psi) = \frac{9-12\cos\psi+3\cos^2\psi+6(1-\cos\psi)(2-2\cos\psi)^{\frac{1}{2}}}{4(2-2\cos\psi)^{\frac{1}{2}}\left[1-\cos\psi+(2-2\cos\psi)^{\frac{1}{2}}\right]^2} \tag{C7}$$

The integration kernel in the second integral of Eq. (22) is simply developed into the form

$$\begin{aligned}\mathscr{L}^{-1}(R,\psi,R+H)\int_{\xi=R+H(\Omega)}^{R+H(\Omega')}\xi^2\,\mathrm{d}\xi &= R^2\left[H(\Omega')-H(\Omega)+\frac{H^2(\Omega')-H^2(\Omega)}{R}\right]\\ &\quad\times\mathscr{L}^{-1}(R+H,\psi,R)+\mathscr{O}\left[\frac{H^3}{R}\right]\end{aligned} \tag{C8}$$

Finally, the truncation coefficients in Eqs. (24) and (25) can be estimated by the 1-D integration over the spherical distance ψ

$$p_n(\psi,\psi_o) = \int_{\psi=\psi_o}^{\pi} \mathscr{M}_1(\psi)[P_n(\cos\psi) - 1]\sin\psi\,d\psi, \quad \forall n = 0,\ldots,nh1 \tag{C9}$$

$$q_n(\psi,\psi_o) = \int_{\psi=\psi_o}^{\pi} \mathscr{M}_2(\psi)P_n(\cos\psi)\sin\psi\,d\psi, \quad \forall n = 0,\ldots,nh1 \tag{C10}$$

$$r_n(\psi,\psi_o) = \int_{\psi=\psi_o}^{\pi} \mathscr{M}_2(\psi)[P_n(\cos\psi) + 1]\sin\psi\,d\psi, \quad \forall n = 0,\ldots,nh2 \tag{C11}$$

$$s_n(H,\psi,\psi_o) = R\int_{\psi=\psi_o}^{\pi} \mathscr{L}^{-1}(R+H,\psi,R)[P_n(\cos\psi) - 1]\times\sin\psi\,d\psi, \quad \forall n \geq 0 \tag{C12}$$

Acknowledgements. The research described in this paper was prepared to meet the objectives of the research contract 'Theoretical and Practical Refinements of Precise Geoid Determination Methods' between Natural Resources Canada and the University of New Brunswick. We thank Natural Resources Canada for their financial support and for providing us with all necessary gravity and elevation data. Additional support was provided by the NSERC of Canada through an operating grant, by a NATO linkage grant, and by the GEOIDE Network of Excellence (project no. 10). A part of the presented research was presented at the CGU Annual Meeting in Banff, May 1999. It also represents a part of the Ph.D. dissertation of the senior author. The authors would also like to acknowledge the thoughtful comments of Prof. P. Holota, Prof. C. Jekeli, Prof. B. Heck and other anonymous reviewers.

References

Gradshteyn IS, Ryzhik IM (1980) Tables of integrals, series, and products. Academic Press, New York

Heck B (1992) A revision of Helmert's second method of condensation in the geoid and quasi-geoid determination. 7th IAG Int Symp Geodesy and Physics of the Earth, IAG-Symposium, No.112. Potsdam, 5–10 October

Heiskanen WA, Moritz H (1967) Physical geodesy. WH Freeman, San Francisco

Martinec Z, Vaníček P (1994a) Direct topographical effect of Helmert's condensation for a spherical approximation of the geoid. Manuscr Geod 19: 257–268

Martinec Z, Vaníček P (1994b) Indirect effect of topography in the Stokes–Helmert technique for a spherical approximation of the geoid. Manuscr Geod 19: 213–219

Martinec Z (1998) Boundary-value problems for gravimetric determination of a precise geoid. Lecture notes in Earth Sciences 73. Springer, Berlin Heidelberg New York

Martinec Z, Matyska C, Grafarend EW, Vaníček P (1993) On Helmert's 2nd condensation method. Manuscr Geod 18: 417–421

Molodenskij MS, Eremeev VF, Yurkina MI (1960) Methods for study of the external gravitational field and figure of the Earth [translated from Russian by the Israel Program for Scientific Translations, Office of Technical Services, Department of Commerce, Washington, DC, 1962]

Nahavandchi H (2000) The direct topographical correction in gravimetric geoid determination by the Stokes–Helmert method. J Geod 74: 488–496

Nahavandchi H, Sjöberg LE (1998) Terrain corrections to power H^3 in gravimetric geoid determination. J Geod 72: 124–135

Novák P (2000) Evaluation of gravity data for the Stokes–Helmert solution to the geodetic boundary-value problem. Tech rep 207, Department of Geodesy and Geomatics Engineering, University of New Brunswick, Fredericton

Sjöberg LE, Nahavandchi H (1998) On the indirect effect in the Stokes–Helmert method of geoid determination. J Geod 73: 87–93

Vaníček P, Martinec Z (1994) The Stokes–Helmert scheme for the evaluation of a precise geoid. Manuscr Geod 19: 119–128

Vaníček P, Huang J, Novák P, Pagiatakis S, Véronneau M, Martinec Z, Featherstone W (1999) Determination of boundary values for the Stokes–Helmert problem. J Geod 73: 180–192

Vaníček P, Novák P, Martinec Z (2001) Geoid, topography, and the Bouguer plate or shell. J Geod 75: 210–215

Wichiencharoen C (1982) The indirect effects on the computation of geoid undulations. Rep 336, Department of Geodetic Science and Surveying, The Ohio State University, Columbus

Wieser M (1987) The global digital terrain model TUG'87. Internal report on set-up, origin, and characteristics. Institute of Mathematical Geodesy, Technical University, Graz